

Remote Sensing for Regional Lake Water Quality Assessment: Capabilities and Limitations of Current and Upcoming Satellite Systems

Leif G. Olmanson, Patrick L. Brezonik, and Marvin E. Bauer

Contents

1	Introduction	112
2	Rationale for Optical Remote Sensing Using Satellite Imagery	113
2.1	Inherent and Apparent Optical Properties and the Radiative Transfer Equation ...	114
2.2	Water Quality Variables Amenable to Measurement by Optical Remote Sensing	115
3	Current and Upcoming Remote Sensing Systems for Regional Water Quality Assessment	126
3.1	Empirical and Semi-analytical Approaches to Lake Water Quality Assessment ...	131
4	Regional Lake Water Quality Assessment: Case Studies	132
4.1	Water Quality of Inland Lakes	132
4.2	Geospatial and Temporal Analysis of Minnesota's 10,000 Lakes	133
5	Conclusions	134
	References	135

Abstract Remote, satellite-based sensing is a cost-effective way to gather information needed for regional water quality assessments in lake-rich areas. A major advantage is that it enables retrieval of current and historic information on lakes that were not part of ground-based sampling programs. Advances over the past decade have enabled the use of satellite imagery for regional-scale measurement of lake characteristics, such as clarity and chlorophyll. For example, in the Midwest USA,

L.G. Olmanson (✉) • M.E. Bauer
Department of Forest Resources, University of Minnesota, St. Paul, MN, USA
e-mail: olman002@umn.edu

P.L. Brezonik
Department of Civil, Environmental, and Geo-Engineering, University of Minnesota,
Minneapolis, MN, USA

historic and recent Landsat water clarity assessments have been conducted on more than 20,000 lakes to investigate spatial and temporal patterns and explore factors that affect water quality. The spatial characteristics of Landsat imagery allow for the assessment of all lakes larger than ~4 ha, but the broad nature and placement of its spectral bands have limited assessments largely for water clarity. European Space Agency (ESA) MERIS imagery with spectral bands that were selected for water has been used to assess chlorophyll for about 900 of Minnesota's large lakes (those > 150 ha). Improvements of the recently launched Landsat 8 and upcoming ESA Sentinel-2 satellites will expand our capabilities further enabling assessment of other optically related water quality characteristics, such as chlorophyll, colored dissolved organic matter (CDOM), and mineral suspended solids for all lakes, and upcoming Sentinel-3 will continue these capabilities for large lakes.

Keywords CDOM • Chlorophyll *a* • Lake water quality • Satellite imagery
Landsat • Secchi depth • Sentinel

1 Introduction

Inland water bodies, such as lakes and reservoirs, are important natural resources for sustenance, recreation, and aesthetic enjoyment, and they add to the economic vitality and quality of life of regions where they occur. Water quality properties, such as chlorophyll *a*, total suspended matter, turbidity, colored dissolved organic matter (CDOM), and nutrients, are used by regulatory and resource management agencies to guide management and public safety decisions. In situ point sampling is the conventional method for collecting information on water quality variables. For effective lake management, it is important to have long-term water quality information on a synoptic scale. The “big picture” view of water quality allows managers to take into account not only differences among lakes but also changes through time for the whole lake and surrounding water bodies within a watershed or typically much larger areas. Unfortunately, only a small percentage of inland waters are regularly monitored by conventional methods, and historical water quality data are lacking for most inland waters. The “big picture” view of water quality is not practical with conventional point sampling methods due to limited resources, and historic water quality data are sparse. Satellite remote sensing has become a viable option for current synoptic measurements and historic assessments of important water quality variables due to improved computer software and hardware, as well as the availability of free or inexpensive satellite imagery.

2 Rationale for Optical Remote Sensing Using Satellite Imagery

Satellite remote sensing has the potential to provide synoptic and frequent water quality measurements of inland waters. Remote sensing satellites such as the Landsat series have been collecting and archiving imagery regularly since the early 1970s, which allows for the assessments of some historic water quality information even on inland waters lacking historical ground-based data. Satellite systems planned for launch in the next few years will allow better characterization of inland water quality on regional-to-global scales.

Optical remote sensing (ORS) using satellite imagery can be used to measure water quality of inland, marine, and coastal waters. Although there are many similarities between ORS applied to inland waters and ORS applied to marine systems, there also are profound differences. For example, spatial resolution requirements are much lower for the broad expanses of the oceans and most coastal areas than are needed for small inland water bodies. Several generations of satellite sensors acquire images with large pixel sizes (~0.3–1 km) that provide adequate spatial resolution for oceanic and most coastal studies but are too coarse for small inland water bodies. For perspective, the smallest water body that can be measured by a satellite sensor with a pixel size of 1 km is ~1,000 ha [1]. The spatial resolution of Landsat satellites, 30 m, generally allows measurements on water bodies larger than ~4 hectares (ha). As pixel size increases, the likelihood decreases that an image will have at least one pixel (preferably four or more) focused solely on open water and not affected by terrestrial and shallow near-shore areas. The smaller pixel size also allows for better characterization of bays and narrow portions of complex lake systems

A second difference relates to the optical complexity of inland waters. Remote sensing scientists focusing on marine systems are able to use increasingly sophisticated instrumentation such as the Moderate Resolution Imaging Spectroradiometer (MODIS) aboard the Aqua and Terra satellites to develop analytical and semi-analytical algorithms that retrieve chlorophyll levels from the oceans, and this has become a routine, global-scale operation [2, 3]. Remote sensing scientists focusing on inland waters have had to develop procedures primarily using other satellites like Landsat, which have adequate spatial resolution but at the same time have critical deficiencies in spectral and temporal resolution. The blue and green spectral bands used to retrieve chlorophyll levels from oceanic waters are not so useful for such purposes in optically complex inland waters [4–7]. These deficiencies have limited development of retrieval algorithms for inland water quality variables by satellite imagery mostly to empirical and semiempirical (described in Sect. 3.1) approaches. More sophisticated ground-based and aircraft-mounted spectroradiometers also have been used in recent years to advance the science of inland water ORS. In summary, the requirements for spatial resolution, most effective spectral bands, ability to use analytical (versus empirical) approaches, and ranges of interest for water quality variables like chlorophyll and CDOM are different between inland

waters and marine systems; these differences resulted in the development of two closely related but separate fields of study (e.g., also see [8]).

2.1 Inherent and Apparent Optical Properties and the Radiative Transfer Equation

When a photon of light interacts with matter, it can either disappear (energy converted to heat or a chemical bond), which is called absorption, or it can change its direction and/or energy, which is called scattering. The absorption and scattering properties of natural waters are the basis for use of ORS in measurement of inland water quality and can be expressed in terms of inherent optical properties (IOPs) and apparent optical properties (AOPs). IOPs depend only on the water medium and are independent of the available light field. Three important IOPs relative to ORS are the absorption coefficient, volume scattering function, and beam attenuation coefficient, all of which are wavelength dependent. The beam attenuation coefficient “c” is the sum of terms for the absorption “a” and scattering “b” of light in the medium:

$$c(\lambda) = a(\lambda) + b(\lambda) \quad (1)$$

where (λ) means a term is a function of wavelength; both $a(\lambda)$ and $b(\lambda)$ are functions of the nature and concentrations of substances in natural waters.

AOPs depend on the IOPs and also on the directional structure of the ambient light field in the medium. The most important AOPs relative to ORS are the irradiance reflectance and various diffuse attenuation coefficients. Signals received by satellite sensors for ORS ultimately get converted to irradiance reflectance values and to a closely related property called “remote sensing reflectance,” hereafter referred to as R_{rs} . Radiative transfer theory provides the connection between IOPs and the AOPs [9] and thus is the basis for relating R_{rs} to concentrations of substances in water that affect light absorption and/or light scattering. The basic radiative transfer equation is [10, 11]:

$$R_{rs} = G(\lambda) \frac{b_b(\lambda)}{a(\lambda) + b_b(\lambda)} \quad (2)$$

where

$$a(\lambda) = a_w + a_{ph}^*(\lambda)C_{chl a} + a_{CDOM}(\lambda) + a_{NAP}^*(\lambda)C_{NAP} \quad (3)$$

and

$$b_b(\lambda) = 0.5b_w(\lambda) + b_{b,ph}^*(\lambda)C_{chl a} + b_{b,NAP}^*(\lambda)C_{NAP} \quad (4)$$

$G(\lambda)$ is a scaling factor accounting for geometrical conditions (e.g., solar zenith angle) and the state of the air-water interface; $a(\lambda)$ is the total absorption coefficient, which is the sum of absorption coefficients for water itself, phytoplankton, CDOM, and non-algal particles (NAP); $a_{ph}^*(\lambda)$ is a chlorophyll-specific absorption coefficient for phytoplankton; $C_{chl a}$ is the concentration of chlorophyll a ; $a_{NAP}^*(\lambda)$ is the specific absorption coefficient for NAP; C_{NAP} is the concentration of NAP; and $b_b(\lambda)$ is the total backscattering coefficient, which similarly is composed of scattering terms for water itself, phytoplankton, and NAP. The backscattering coefficient for pure water is equal to one-half of the total scattering coefficient of pure water; it is assumed that there is equal probability of scattering in the forward and backward directions [11]. Equations (2)–(4) assume that the absorption and scattering properties of a water body depend on contributions from four components: pure water, phytoplankton, CDOM, and NAP. Ultimately, analytical and semi-analytical models for retrieval of water quality information on these variables are based on these equations.

2.2 *Water Quality Variables Amenable to Measurement by Optical Remote Sensing*

2.2.1 *Currently Measured Variables*

To be measurable by ORS, a water quality constituent must affect at least one of the two principal optical properties that control the amount of light reflected back to a sensor from the water body: absorption and scattering. Because pure water strongly absorbs incoming radiation in the ultraviolet (UV) range and also (but to a somewhat lesser extent) in the infrared (IR) range, the portion of the electromagnetic spectrum useful for remote sensing of water quality is limited to the visible range (~400–700 nm) plus the near UV (roughly 360–400 nm) and the near IR (~700–900 nm). Beyond this range, absorption of incoming radiation is so strong that essentially nothing is reflected back into the atmosphere. Consequently, the water quality constituents amenable to measurement by ORS must absorb or scatter light within this wavelength range.

Constituents like plant pigments, especially chlorophyll a , and humic substances, which constitute much of the CDOM in water bodies, are the most important examples of light-absorbing substances amenable to measurement by ORS. CDOM is usually reported by limnologists and remote sensing scientists in terms of its light absorptivity at specific wavelengths, commonly 420 and 440 nm, e.g., a_{440} (m^{-1}), but chlorophyll units (CPU) are still used by some water quality

scientists and engineers. Although many synthetic organic compounds used in modern society are colored (i.e., absorb light in the visible range), they do not occur in natural waters at sufficient concentrations, except in very rare pollution events, to be measurable by ORS. Similarly, a variety of metal ions and metal-ion complexes are visibly colored (e.g., species of Cr, Cu, and Mn), but their concentrations in natural waters, especially in forms that are colored, are far too low to affect reflectance spectra. A possible exception, iron (Fe), is discussed below in the context of CDOM measurements.

Suspended particles, including phytoplankton, organic detritus derived from microbial decomposition and secondary production, and mineral suspended solids such as aluminosilicate clays and soil particles (SS_{\min}), are the primary constituents in natural waters that affect scattering. Because the spectral characteristics of light scattering by various types of suspended particles are not sufficiently unique, ORS techniques generally are not able to distinguish among the types of suspended particles causing scattering and thus affecting reflectance. Phytoplankton cells, because of their chlorophyll content, are an exception, but results normally are presented in terms of chlorophyll concentrations and not cell counts or cell volume. Light-scattering water quality constituents measured by ORS thus are “lumped parameters” like total suspended solids (TSS) and turbidity. Light scattering depends on a complicated set of factors, including particle numbers, sizes, shapes, and surface properties; no universal relationship between the reflectance of light and TSS (in mg/L) thus should be expected. Rather, such relationships are time and place specific depending on the properties of the suspended particles, as mentioned above. Because turbidity measured by a laboratory turbidimeter or nephelometer is directly related to the scattering of light in water bodies that produces the reflected light measured by optical remote sensors, development of universal or quasi-universal ORS relationships for turbidity may be possible. A few studies have reported on the measurement of turbidity by ORS and are discussed further in Sect. 2.2.4.

Secchi depth (SD), an important optical property of natural waters, is affected by both light scattering and light absorption. In most water bodies, scattering caused by phytoplankton and plankton-derived particles controls SD, and thus it serves as a common and simple measure of lake trophic status. Many studies have shown strong correlations between SD^{-1} and chlorophyll levels (or log SD versus log [chlorophyll]) in lakes [1, 12]. CDOM and SS_{\min} also affect SD in some waters, and proper interpretation of SD data depends on what factors are affecting water clarity. Brezonik [13] quantified the influence of CDOM on SD using in situ experiments in which a concentrated source of CDOM-like material was added incrementally to low-CDOM and low turbidity lake water in mesocosm-scale “limnobags.” At a measured CDOM of 200 CPU, equivalent to $a_{440} \approx 20 \text{ m}^{-1}$, representative of highly colored bog lakes, and negligible SS_{\min} , the SD was $\sim 1.5 \text{ m}$; at CDOM = 70 CPU ($a_{440} \approx 7 \text{ m}^{-1}$), representative of moderately colored lakes, the SD was 4.5 m. Preisendorfer [14] showed that SD^{-1} is proportional to the sum of two fundamental optical properties: $\alpha + K_d$, where α is the beam attenuation coefficient (measured by an underwater transmissometer) and K_d , the diffuse attenuation coefficient

(determined by measuring the amount of incident light remaining as a function of depth with an underwater light meter). K_d and α are spectrally and depth averaged values for a given water body.

Values of K_d at specific wavelengths, most commonly $K_{d,490}$, have been retrieved from ORS data by marine scientists as part of efforts to develop analytical methods to retrieve water quality information from satellite imagery (e.g., [10, 15, 16]). Plug-in algorithms to compute $K_{d,490}$ were developed for several MERIS processors in the BEAM software system, including the Case 2 Regional and Boreal lakes processors [17–19]. K_d is not a common water quality variable in inland waters, however, and there seems to have been little interest among freshwater remote sensing scientists in using the algorithms for K_d in inland lakes. This situation is likely to change when improved satellite sensors (see Sect. 2) that allow for more analytical retrieval methods become available for inland water ORS measurements.

In summary, only a few water quality variables are amenable to direct measurement by ORS, but they include two variables, chlorophyll a and CDOM, that are critically important for understanding lake metabolism and carbon cycling. A third variable, SD, probably is the most widely measured lake water quality parameter because its simplicity and low cost facilitates use by citizen monitoring programs. SD also is important because it is related directly to water quality as perceived by lake users and to trophic conditions and chlorophyll levels. TSS and turbidity round out the common water quality variables amenable to measurement by ORS.

2.2.2 Potential Variables with Improved Spectral Characteristic Sensors

As noted above, a few other variables could become important in applications of ORS to regional-scale measurements of inland lake water quality when sensors with improved spectral characteristics and adequate spatial resolution become available. These include SS_{min} , K_d , and specific plant pigments indicative of various classes of algae (e.g., see [10]), such as phycocyanin for cyanobacteria. Identification and measurement of the abundance of submerged and emergent aquatic plants also can be achieved using ORS [20–22], but details of this topic are beyond our scope.

2.2.3 Non-optical Variables Sometimes Correlated with Variables Having Optical Properties

Many examples can be found in the remote sensing literature that claim the ability to measure water quality variables that do not directly affect light reflectance or are present in natural waters at such low concentrations that they do not affect reflectance signals measured by satellite sensors. Examples include mercury, bacteria (e.g., *Escherichia coli*) [23], and total phosphorus (TP) [24, 25]. In all cases, the reported relationships involve empirical regression equations. Despite the fact that

high r^2 values sometimes are reported, the relationships “work” only because the “non-optical” variable is correlated in the water bodies used to develop the relationship with an optical variable that affected reflectance. For example, the bacterial indicator of fecal contamination, *E. coli*, is found in waters contaminated by human activities, and correlation of *E. coli* abundance with TSS and turbidity might be expected. Similarly, phosphorus often is the limiting nutrient for algal growth in lakes, and correlations between chlorophyll and TP or SD and TP thus are common (e.g., [12]). Such relationships cannot be applied reliably beyond the database from which they were derived because no intrinsic or causative relationship exists between the non-optical and optical variables or between the non-optical variable and reflectance.

The use of empirical relationships that depend on secondary correlations has led to criticisms that remote sensing scientists are “overselling” their technology (e.g., [8, 26]). A more transparent and defensible approach is to develop relationships between reflectance data and variables that directly affect reflectance and then separately determine whether a sufficiently close relationship exists between the optical variable retrieved from imagery and a non-optical variable of interest. Applications of such empirical relationships still should be limited to the data sets on which they are based, but situations exist in which useful information can be obtained by this approach. For example, evaluation of a suite of environmental conditions retrieved from satellite imagery was found useful in predicting outbreaks of waterborne diseases even though the disease-causing microorganisms do not directly affect satellite imagery signals [27]. Similarly, atmospheric scientists have estimated transport of specific pollutants like mercury (Hg) from Asia across the Pacific Ocean to North America by tracking atmospheric dust using satellite imagery and independent measurements of the pollutant (e.g., Hg) concentrations in atmospheric dust over the Pacific.

Relationships between DOC (dissolved organic carbon) and reflectance also have been reported (e.g., [28]), but insofar as DOC per se is not an optical variable and does not itself affect reflectance, these also are the results of indirect correlations. To the extent that such relationships work, they rely on the fact that a fraction of DOC (CDOM) affects reflectance. For some waters good correlations exist between CDOM and DOC, but as Brezonik et al. [29] recently showed, no single DOC-CDOM relationship applies across a broad spectrum of surface waters. Some sources of DOC, e.g., autochthonous organic matter and anthropogenic organic matter derived from wastewater, have low color per unit of carbon. As a result, CDOM and DOC are poorly correlated in many natural waters. For example, Spencer et al. [30] found that r^2 values for DOC-CDOM relationships were ≤ 0.5 in 11 of 30 large North American rivers, and four rivers (the Colorado, Columbia, Rio Grande, and St. Lawrence) had $r^2 < 0.2$. Factors giving rise to poor DOC-CDOM relationships include the extent to which the DOC is autochthonous or anthropogenic and the extent to which allochthonous DOC has been photodegraded.

The following three sections summarize the spectral basis for retrieval of the three most important water quality characteristics—clarity, chlorophyll, and CDOM—from remote sensing imagery.

2.2.4 Water Clarity Variables

Three water clarity variables discussed here include Secchi depth (SD), turbidity, and TSS.

Water clarity, whether measured as light scattering in laboratory turbidimeters, as the in situ depth of disappearance of a white disk (SD), or as the slope of the logarithm of light attenuation with depth (K_d) in a water body, provides critically important information to both users of water bodies and to water resource managers. Fortunately, because of their close relationship to both IOPs and AOPs of water, clarity parameters are well suited to measurement by ORS.

In part because of the widespread availability of calibration data from citizen and agency monitoring programs, SD has been the subject of many ORS studies (see Sect. 4 for details). Retrieval of SD from satellite imagery also is facilitated by the fact that the broad Landsat bands are suitable for SD retrieval. Numerous studies have yielded good relationships for SD that involve bands 1 and 3 in two-term equations like $\ln(\text{SD}) = a(\text{TM1}/\text{TM3}) + b\text{TM1} + c$ [31], where $\ln(\text{SD})$ is the natural logarithm of Secchi depth; a , b , and c are regression coefficients; and TM1 and TM3 are reflectance values for thematic mapper bands 1 and 3. As SD decreases, reflectance in the red band (TM3) increases. The blue band (TM1) tends to normalize brightness in the red and improves algorithm performance. R^2 values for such equations are in the range 0.71–0.96 for lakes in Minnesota [32]; others [33] reported similar ranges of fit. Olmanson et al. [1] found that MERIS and Landsat imagery worked equally well for SD, but the coarser spatial resolution of MERIS allowed assessment of only about 8 % of the Minnesota lakes accessed by Landsat.

Models for turbidity and TSS in optically complex waters, where phytoplankton, CDOM, and SS_{min} all may affect IOP features, should avoid the absorption characteristics of chlorophyll in the red and CDOM in the blue region and use the scattering peak at ~705 nm or band combinations in the NIR or green regions (where plant pigments have minimal absorption). For example, Gitelson et al. [34] found that a difference ratio algorithm $(R_{560} - R_{520})/(R_{560} + R_{520})$ was highly correlated with TSS in lakes and rivers with TSS values < 66 mg/L. Phytoplankton absorption is at a minimum near 560 nm, but reflectance at this wavelength is sensitive to TSS; in contrast, reflectance at 520 nm is relatively insensitive to changes in TSS [35].

Numerous studies have shown the usefulness of NIR bands for turbidity and TSS (for reviews, see [10, 35]). The scattering peak at ~700 nm was found to be strongly correlated with TSS by many studies (e.g., [36–38]), and Senay et al. [39] reported a good relationship for turbidity. The difference in reflectance at 710 and 740 nm was

found useful by Shafique et al. [40]. The scattering peak at ~ 700 nm by itself also was found to work well for NVSS (nonvolatile SS, essentially equivalent to SS_{\min}) [41].

Olmanson et al. [42] found strong relationships between reflectance at 705 nm and both turbidity and TSS ($r^2 = 0.77\text{--}0.93$ for both) using airborne hyperspectral imagery to assess water quality in the optically complex waters of the Minnesota, Mississippi, and St. Croix Rivers in the Minneapolis-St. Paul region. Depending on location and time, CDOM, phytoplankton, and/or SS_{\min} all may dominate the optical properties of these rivers. They also found a predictive equation ($r^2 = 0.80\text{--}0.90$) for volatile suspended solids, VSS, a measure of organic suspended matter, using the ratio of reflectance at 705 to 670 nm. For SS_{\min} they found that using band at 705 nm and the ratio of reflectance at 705 to 670 nm, a combined model (TSS and chlorophyll *a*), yielded an r^2 of 0.85–0.97 for SS_{\min} . The resulting maps clearly distinguished phytoplankton-based turbidity from SS_{\min} (Fig. 1 [42]; reprinted with permission from the publisher). The transition from phytoplankton-dominated water at location “a” (Fig. 1B) to inorganic sediment-dominated water at location “e” is captured in the reflectance spectra extracted from the imagery (Fig. 2). Absorption characteristics of chlorophyll are distinctly visible at location “a” but become more moderate toward location “e.” This example demonstrates the massive quantity of information obtainable from a single image that would have been missed by traditional monitoring, which would probably involve only one sample for the entire area.

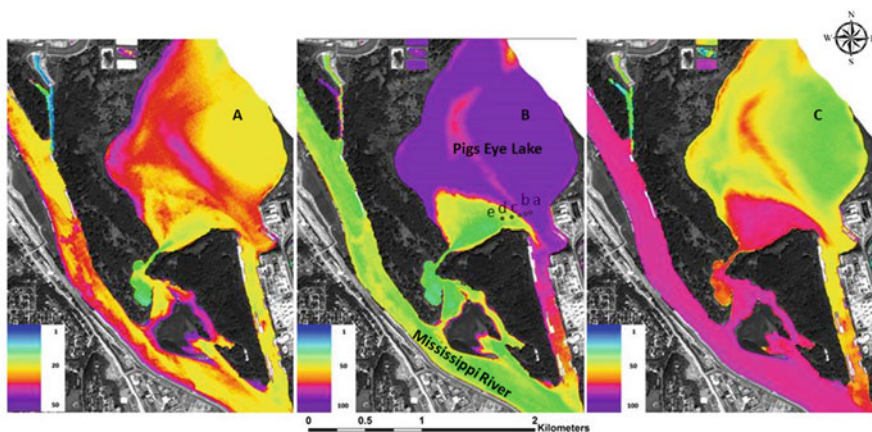


Fig. 1 Maps of Pig’s Eye Lake, St. Paul, Minnesota, showing transition from conditions dominated by inorganic sediment to conditions dominated by phytoplankton: (A) turbidity, (B) chlorophyll *a*, and (C) NVSS/TSS (% SS_{\min}); August 30, 2007. Reprinted from Olmanson et al. [42] with permission of the publisher

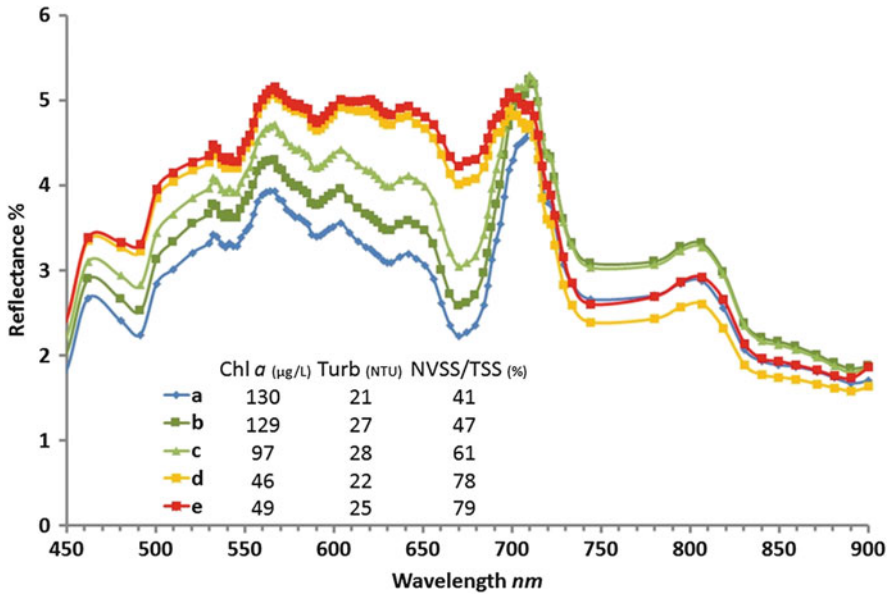


Fig. 2 Reflectance spectra of the transition zone for conditions dominated by inorganic sediment in the Mississippi River to conditions dominated by phytoplankton in Pig's Eye Lake, August 30, 2007 (Fig. 1b). Tabulated chl *a*, turbidity, and NVSS/TSS values were calculated from reflectance spectra using the best predictive models. Reprinted from Olmanson et al. [42] with permission of the publisher

2.2.5 Chlorophyll and Other Pigments

Predictive models that use ORS to estimate a water quality variable should use wavelengths that identify key spectral characteristics of the variable without interference from competing optical features of other variables. For chlorophyll, this means that algorithms commonly used for the open oceans, which involve reflectance in the blue and green regions, do not work well for inland waters because these waters are influenced by TSS and CDOM. This makes them optically more complex [43] than open ocean waters, where chlorophyll and chlorophyll-related properties are the primary factors affecting reflectance. CDOM and SS_{min} have overlapping absorption features with chlorophyll *a* in the blue region.

Successful chlorophyll models for inland waters thus use absorption characteristics in the red wavelengths—a reflectance trough at ~670 nm caused by a peak in absorption by chlorophyll *a* and a reflectance peak at the red edge (~700–710 nm) caused by scattering by phytoplankton; absorption by CDOM and suspended solids is minimal at these wavelengths [44, 45]. Many studies (e.g., [34, 46–50]) have reported strong relationships between chlorophyll *a* and the reflectance ratio for ~700 nm and ~670 nm in a variety of inland waters and over a wide range of concentrations (e.g., 0.1–350 µg/L; [35]). The usefulness of the red-edge signal for chlorophyll *a* estimation in optically complex river waters also was shown by

Olmanson et al. [42] using airborne hyperspectral imagery on waters of the Minnesota, Mississippi, and St. Croix Rivers. For chlorophyll *a*, the ratio of reflectance at 705 to 670 nm yielded r^2 values of 0.75–0.93. Of the recently or currently available and forthcoming satellite sensors, only MERIS and the Sentinel-2 and Sentinel-3 satellites have appropriately narrow red-edge bands.

Despite the above comments, it must be noted that many studies have reported strong empirical relationships between the broad bands of Landsat sensors and chlorophyll *a* (e.g., [1]); typical predictive equations involve the ratio of TM or ETM+ bands 1 and 3. Absorption by chlorophyll *a* is strong in bands 1 (450–520 nm) and 3 (630–690 nm). Nonetheless, increased scattering by phytoplankton cells counteracts some of the absorption effects and leads to increased reflectance with increasing chlorophyll *a* levels in band 1 and even larger increases in band 3. If it is known that the optical properties of the water bodies being studied are dominated by phytoplankton, the use of these empirical relationships may be considered acceptable. However, for regional assessments where specific water quality characteristics are not known, lakes with high CDOM and/or SS_{\min} may be misclassified.

As an example, when we used Landsat 8 imagery to estimate chlorophyll *a* and SD in lakes of northeastern Minnesota for August 31, 2013, we found strong relationships for both variables ($r^2=0.70$ and 0.77 ; RMSE 0.758 and 0.406 , respectively). Calibration data (± 3 days) for the images are from the Minnesota Pollution Control Agency (for chlorophyll *a*, $n=99$; for SD, $n=258$) [51]. For most Minnesota lakes, the results are believed accurate because phytoplankton dominates their optical properties. When we used the same models for the St. Louis River Estuary (SLRE), where optical properties of the waters are dominated by CDOM and SS_{\min} , however, the resulting maps misrepresented SS_{\min} as chlorophyll (Fig. 3 zoomed into Duluth, MN & Superior, WI area: SLRE at the western edge of Lake Superior). Consequently, we believe it is best to limit regional-scale assessments using Landsat to water clarity or turbidity, which is appropriate for the spectral characteristics of the Landsat sensors, unless independent data are available to verify that SS_{\min} and CDOM are not important factors in the lakes being assessed.

The characteristics of Landsat, MERIS, and MODIS sensors for regional water quality measurements were analyzed by Olmanson et al. [1]. Imagery from the three sensors was compared for spatial and spectral characteristics, and empirical models were developed for chlorophyll *a* using various bands and band ratio combinations as dependent variables. MERIS provided a better fit for chlorophyll *a* ($R^2=0.85$, $n=90$) than Landsat and MODIS ($R^2=0.79$ for both, $n=177$ and 42 , respectively). The red-edge band at 708 nm improved the fit and allowed discrimination between phytoplankton and SS_{\min} , but the Landsat and MODIS results misclassified high SS_{\min} levels as chlorophyll *a*, similar to Fig. 3.

Phycocyanin, a pigment occurring in cyanobacteria (formerly known as blue-green algae), can serve as a marker for the presence of these microorganisms in surface waters and is amenable to measurement by ORS. Cyanobacteria are common in eutrophic water bodies, and some species produce substances that are toxic

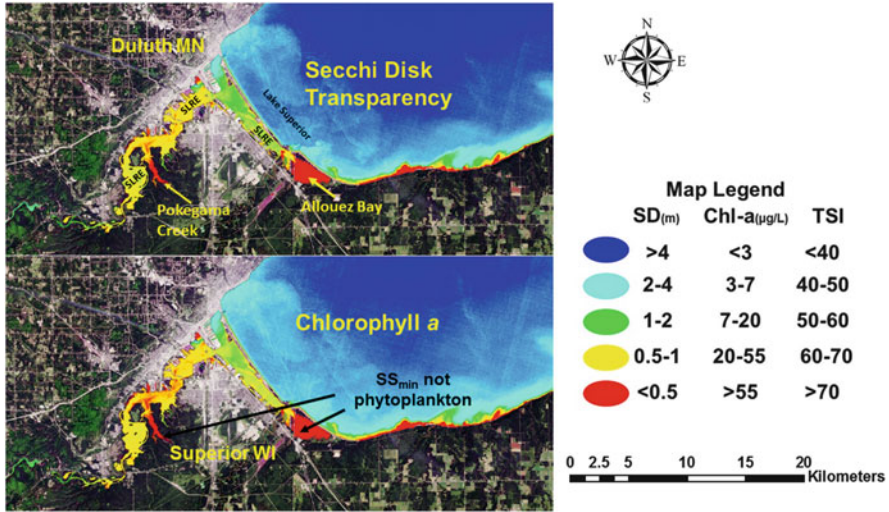


Fig. 3 Maps of chlorophyll *a* and SD in the St. Louis River Estuary (SLRE) at west end of Lake Superior created from an Aug. 31, 2013, Landsat 8 image. Spectral characteristics of the OLI sensor do not allow discrimination of phytoplankton from SS_{min} in optically complex waters. The SS_{min} dominated waters of Pokegama Creek and Allouez Bay are misclassified as having high chlorophyll *a*. Models were developed for the entire path 27 row 27 Landsat image using available lake data, *n* = 260 for SD, 71 for chlorophyll *a* within 3 days of the image

to animals. Thus, there has been much interest by water resource managers in methods for real- or near real-time assessment of the abundance and spatial distribution of cyanobacterial blooms. Phycocyanin has a strong absorption peak near 620 nm, which leads to a characteristic dip in reflectance spectra around 600–630 nm for water bodies with cyanobacteria blooms (e.g., Fig. 4). Several researchers have reported empirical algorithms for cyanobacterial abundance using hyperspectral measurements and reflectance ratios around this wavelength range [52, 53]. Unfortunately, this wavelength range represents a gap in coverage by the sensors of the Landsat satellites (for OLI of Landsat 8, band 3 has a range of 530–590 nm and band 4 a range of 640–70 nm). Vincent et al. [54] claimed to be able to measure phycocyanin and trace cyanobacterial blooms in Lake Erie using Landsat. They reported an *r*² of 0.77 for the relationship, but this is thought to be an example of indirect correlation (e.g., [35]). The retrieval equation probably was responding to chlorophyll signals; cyanobacteria were the dominant algae in the lake at the time of the measurements, and a high correlation could be expected between phycocyanin and chlorophyll levels. Several groups (e.g., [55–58]) have found that the narrower bands of MERIS are suitable for retrieval of phycocyanin concentrations. In these cases, the fluorescence of phycocyanin at ~681 nm is detected using a semiempirical second derivative function that also uses reflectance data for nearby bands at 709 and 665 nm.

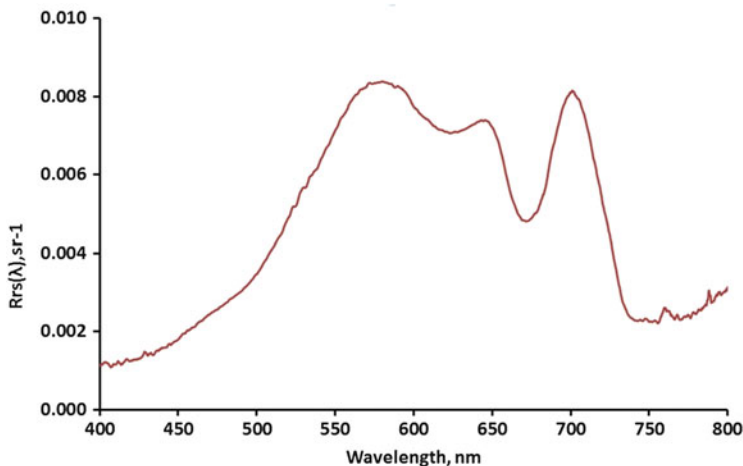


Fig. 4 Reflectance spectra for a eutrophic stretch of the Mississippi River downstream of St. Paul, Minnesota. Data redrawn from Brezonik et al. [29]

2.2.6 Colored Dissolved Organic Matter

Interest among aquatic scientists has increased greatly over the past decade in ORS applications to measure CDOM in surface waters. In part, this reflects a growing interest in quantifying the role of lakes and other surface water bodies in the global carbon cycle, along with the understanding that CDOM represents a large fraction of the total DOC in many aquatic systems.

A wide range of approaches, including analytical, semi-analytical, matrix inversion, and empirical techniques, have been used to retrieve CDOM values for fresh and marine waters by satellite imagery. The most successful algorithms for marine conditions (including coastal waters) involve semi-analytical matrix inversion methods (e.g., [59–61]); but such approaches have been used only a few times for freshwaters (e.g., [11, 62]). The most common retrieval methods for lakes are empirical reflectance-ratio equations that involve nonlinear (power) equations. For example, the equation of Kutser et al. [4] uses the ratio of Advanced Land Imager (ALI) band 2 (525–605 nm) to band 3 (630–690 nm): $a_{420} = 5.13(\text{ALI}2/\text{ALI}3)^{2.67}$. ALI bands 2 and 3 have approximately the same wavelength ranges as Landsat TM and ETM+ bands 2 and 3 and Landsat 8 OLI bands 3 and 4. Menken et al. [49] independently found a similar relationship using ground-based hyperspectral reflectance data, $a_{440} = 146.4(\text{R}_{670}/\text{R}_{550})^{2.08}$, and Ficek et al. [63] also used a similar equation.

Using in situ reflectance hyperspectra and associated water quality measurements on ~30 Minnesota and Wisconsin lakes with wide ranges of CDOM, chlorophyll, and TSS, Brezonik et al. [29] recently found that the best band ratio models used similar wavelengths for Landsat 8 bands. With the larger selection of Sentinel-2 and Sentinel-3 bands, a different ratio using ~500 nm:~750 nm worked best.

Simulated Landsat 8, Sentinel-2, and Sentinel-3 bands calculated from the hyperspectra yielded $r^2 = 0.84\text{--}0.86$ for a_{440} . The broader Landsat 8 bands worked nearly as well as the narrower Sentinel bands and hyperspectral bands, probably because CDOM lacks specific peaks or troughs in absorbance or reflectance. These r^2 values generally are considered very good for remote sensing predictive equations. Nonetheless, the average for absolute values of percent difference between measured and predicted CDOM across the four best predictive models was 31 %. Although some of the differences can be attributed to sampling variability and measurement uncertainty, the largest source likely is model error. Such large uncertainties should serve as a cautionary note to limnologists and remote sensing scientists.

The effectiveness of predictive equations based on longer wavelengths is counterintuitive given that CDOM absorptivity increases quasi-exponentially with decreasing wavelength and is increasingly diminished in the green and red regions. Although the physical basis for the relationships is still uncertain, the higher band (ALI3, OLI4) centered at 670 nm probably corrects for effects of chlorophyll on reflectance, and the lower band (ALI2, OLI3) centered at ~ 560 nm probably measures the influence of CDOM. It is important to realize that the small absorbance values measured in laboratory spectrophotometers involve much shorter light paths (1–10 cm) than those of interest in lakes. For example, as noted earlier, a CDOM level of $a_{440} = 20 \text{ m}^{-1}$ implies a Secchi depth of ~ 1.5 m. Based on UV-visible absorbance spectra we have measured on similar waters, such a sample would have an absorbance (A) of ~ 0.022 at 560 nm in a 1 cm cell. Given that the Beer-Lambert law applies, the value of A that would apply to a light path of 1.5 m would be ~ 3.3 , and converting to percent of incident light at 560 nm remaining at a depth of 1.5 m yields a value of ~ 3 %. Light reflected back to the air-water interface from the white surface of the Secchi disk again must travel 1.5 m through the absorbing medium, and thus much less than 1 % of the incident light at 560 nm arrives back at the water surface. Clearly, even small absorbance values measured in the laboratory have large effects on reflectance when the long light paths of lake water columns are considered.

Brezonik et al. [29] found a CDOM-dependent difference in slopes of reflectance spectra in the range of $\sim 570\text{--}650$ nm. For low-CDOM waters, reflectance decreased with increasing wavelength, but for high-CDOM waters reflectance increased with increasing wavelength. Even though CDOM absorbance is low in this range, it does affect reflectance, as the calculation in the preceding paragraph demonstrated. Other constituents that affect reflectance spectra (notably plant pigments) have minimal effects in this wavelength region.

CDOM levels are much lower in marine waters than in freshwaters; absorptivity at 412 nm, a_{412} , generally is $< 1 \text{ m}^{-1}$ in coastal waters and $< 0.1 \text{ m}^{-1}$ in the open ocean. In contrast, a_{440} values $< \sim 2 \text{ m}^{-1}$ in lakes generally are considered negligible, although remote sensing scientists are starting to take interest in measuring CDOM in low-CDOM lakes [29]. Values in lakes that are considered “humic colored” commonly are in the range of $\sim 5\text{--}20 \text{ m}^{-1}$ and may range up to 40 m^{-1} or even more in highly colored bogs. Concentrations of TSS and chlorophyll also

tend to be higher in freshwaters than in the oceans, and most freshwaters thus are optically very complex. As noted earlier for chlorophyll, remote sensing methods used for marine waters are not always applicable to freshwaters, and this situation also applies to CDOM. For example, marine scientists interested in CDOM look forward to using a band in the near UV (~380 nm) that will be available on a forthcoming NASA sensor for ocean CDOM. Plant pigment absorbance decreases greatly below ~400 nm, but CDOM absorbance continues to increase exponentially. This band thus avoids interference between the absorbance of plant pigments and CDOM that precludes using bands in the blue region for CDOM retrieval. Bands in the near UV likely would not be useful for inland waters, however, because light absorption by the typically higher levels of CDOM is so strong that there is essentially no reflectance signal (all incoming light is absorbed).

Finally, one of the main reasons for measuring CDOM by ORS is the possibility of using the values to estimate DOC in lakes at regional-to-global scales. As discussed in Sect. 2.2.3, this is not straightforward because DOC-CDOM correlations are not always high. Even when they are, a relationship that works well for one set of lakes may not be the same for a different set of lakes. A further complication in DOC-CDOM relationships is the recent finding that complexation of DOM by dissolved iron enhances the color intensity of the organic substances [64, 65]. Scientists interested in using CDOM to estimate DOC at regional-to-global scales should recognize that DOC-CDOM relationships are site specific and perhaps time specific [29]. Additional predictor variables likely will be needed to develop more robust predictive relationships between CDOM and DOC. In addition to a possible need to account for the iron content of the water, water residence time would help account for photobleaching of CDOM [66], the CDOM spectral slope (S) would help define the quality or structural nature of CDOM [67, 68], and various climatic and landscape metrics [69, 70] may account for DOC loadings to lakes.

3 Current and Upcoming Remote Sensing Systems for Regional Water Quality Assessment

A large number of airborne and space-borne sensors are potentially available for remote sensing of water resources (Table 1), but none is ideally suited for monitoring inland waters, especially regarding our primary interest for this chapter—water quality assessments of all lakes (above some nominal size) at regional scales. Systems that are expensive, need to be tasked to collect specific imagery, cover only small areas, or have coarse spatial resolution may be suitable for special projects but not for routine synoptic lake monitoring. Moreover, sensors with only a few broad bands do not provide reflectance data useful for accurate retrieval of water quality measures like chlorophyll across a broad range of water quality conditions, i.e., for optically complex inland waters. Characteristics of systems suitable for regional aquatic assessments include spatial resolution appropriate for lakes > 4 ha (i.e., spatial resolution or pixel size of 5–50 m²), regular collection of imagery

Table 1 Potential space-borne sensors for remote sensing of water resources

Satellite/sensor	Period of operation	Spatial (m)	Resolution				Image cost (\$)	Limitations
			Spectral (no. bands) (Vis/RE/NIR/SWIR/TIR) ^a (no.)	Radiometric (bits)	Temporal (days)	Swath width (km)		
<i>Landsat class</i>								
Landsat 5	1984–2012	30/120	3/0/1/2/1 (7)	8	16	180	Free	Spectral, temporal
Landsat 7	1999–present	30/60	3/0/1/2/1 (7)	8	16	180	Free	Spectral, temporal
Landsat 8	2013–present	30/100	4/0/1/2/2 (10)	12	16	180	Free	Spectral, temporal
Spot-5	2002–present	10/20	3/0/1/0/0 (4)	8	26 nadir, 2–3	60	\$	Spectral, cost
Spot-6	2012–present	6	3/0/1/0/0 (4)	12	26 nadir, 2	60	\$\$	Spectral, cost
Spot-7	2014–present	6	3/0/1/0/0 (4)	12	26 nadir, 2	60	\$\$	Spectral, cost
RapidEye	2008–present	5	3/1/1/0/0 (5)	12	5.5 nadir, 1	77	\$	Spectral, cost
<i>High resolution</i>								
IKONOS	1999–present	3.2	3/0/1/0/0 (4)	11	3.5	11.3	\$\$	Spectral, cost
QuickBird	2001–present	2.44	3/0/1/0/0 (4)	11	3	16.5	\$\$	Spectral, cost
GeoEye-1	2008–present	1.65	3/0/1/0/0 (4)	11	26 nadir, 4–5	15.2	\$\$	Spectral, cost
WorldView-2	2009–present	1.85	5/1/2/0/0 (8)	11	1.1 off nadir	16.4	\$\$\$	Cost, swath
WorldView-3	2014–present	1.24/3.7/30	9/1/5/13/0 (28)	11	4.5 off nadir	66 (5 strips)	\$\$\$\$	Cost

(continued)

Table 1 (continued)

		Resolution							
Satellite/sensor	Period of operation	Spatial (m)	Spectral (no. bands) (Vis/RE/NIR/SWIR/TIR) ^a (no.)	Radiometric (bits)	Temporal (days)	Swath width (km)	Image cost (\$)	Limitations	
<i>Oceanographic</i>									
CZCS	1978–1986	825	4/0/1/1/0 (6)	8	Varies	1,566	Free	Spatial, spectral	
SeaWiFS	1997–2010	1,100	6/0/1/1/0 (8)	10	1	2,801	Free	Spatial, spectral	
MODIS Terra	1999–present	250/500/1 km	10/0/6/14/6 (36)	12	1	2,330	Free	Spatial, spectral	
MODIS Aqua	2002–present	250/500/1 km	10/0/6/14/6 (36)	12	1	2,330	Free	Spatial, spectral	
<i>Hyperpectral</i>									
HICO	2009–present	~90	52/2/33/0/0 (87)	12	Varies	42 × 192	Free	Experimental, limited images	
Hyperion	2000–present	30	34/2/43/163/0 (220)	12	Varies	7.5 × 100	Free	Experimental, limited images	
<i>Approaching ideal</i>									
MERIS	2002–2012	300	8/1/6/0/0 (15)	12	3	1,200	Free	Spatial, no SWIR for atm corr	
Sentinel-2	Planned 2015	12/20/60	4/1/5/3/0 (13)	12	5	290	Free	Spectral but has red edge	
Sentinel-3 (OLCI)	Planned 2015	300	10/1/10/0/0 (21)	12	2.8	1,269	Free	Spatial	

This is not an exhaustive list of satellite sensors that provide monitoring capabilities for aquatic resources but includes the ones that have been used most widely or show the greatest promise for future use

^aVis visible, RE red edge, NIR near infrared, SWIR shortwave infrared, TIR thermal infrared

(preferably at least weekly but every 2–3 days is better), appropriate spectral bands (discussed further below), and images that are inexpensive or available for free. As Table 1 indicates, all current sensors fail to meet one or more of these criteria. The Medium Resolution Imaging Spectrometer (MERIS) sensor on the European satellite Envisat came closest to meeting the above criteria, but it has not been operational since 2012, and its pixel size (300 m²) limited it to moderately large lakes (> 150 ha [~370 ac]). For Minnesota, its spatial resolution provided measurements for only ~8 % of the state’s lakes [1].

This situation leaves Landsat and related satellites (Table 1) as the current “default systems” for inland lake monitoring by ORS. The Landsat series was designed primarily for land features and has been hugely important for land use/land cover analyses, vegetation condition, and agricultural applications, but Landsat sensors also have been used for over 30 years to estimate some water quality variables on inland lakes [71–76]. The biggest drawback of the Landsat sensors, aside from low temporal resolution (repeat coverage every 16 days), is their limited and coarse spectral resolution (only 3–4 bands in the visible range (e.g., for Landsat 5 and 7: band 1, 450–520 nm; band 2, 520–600 nm; band 3, 630–690 nm; Landsat 8 added a new band 1, 430–450 nm, and slightly narrowed the ranges for the earlier three bands, which now are designated band 2 through band 4). As described in Sect. 2.2.5, this may hinder the accurate retrieval of data on important variables like chlorophyll in waters with complex optical properties and also limits the types of algorithms applicable to Landsat data.

A class of multispectral sensors with high spatial resolution (Table 1) could be used for more locally based regions, such as city-scale projects. This imagery can be fairly expensive, but for important areas and projects, it has the advantage of being able to monitor smaller water bodies than Landsat can. For example, Sawaya et al. [21] found that IKONOS imagery worked as well as Landsat for water clarity (SD) assessment, and a single image was able to assess the clarity of 236 lakes and ponds as small as 0.08 ha in the City of Eagan, Minnesota. In contrast, Landsat imagery was able to assess only 48 of the water bodies (minimum size of 1.5 ha). The spatial resolution of IKONOS and QuickBird images has made them particularly useful for aquatic plant surveys [21, 22]. Several high-resolution systems are now operational (Table 1), but WorldView-2 and WorldView-3 with 8 and 28 spectral bands, respectively, may be particularly useful for water quality assessments.

Launched in February 2013 with a new Operational Land Imager (OLI) sensor, Landsat 8 has several improvements over the Thematic Mapper (TM) and Enhanced Thematic Mapper (ETM+) instruments on previous Landsat satellites. The OLI sensor has improved signal-to-noise ratio, radiometric resolution (12-bit vs. 8-bit for Landsat 5 and 7), and two new spectral bands—a shorter wavelength blue band (see above) and a shortwave infrared band positioned to detect cirrus clouds. These advancements should improve the ability to map variables like water clarity and CDOM but may not improve the discrimination of chlorophyll from SS_{min}. Landsat 7 launched in 1999 continues to collect imagery and can be used for water clarity assessments.

US government agencies have made significant investments in systems like the Coastal Zone Color Scanner (CZCS), Sea-viewing Wide Field-of-view Sensor

(SeaWiFS), and MODIS, to monitor oceans and coastal areas. Each sensor yielded advances in sensor technology, and as noted earlier, they provide useful information on chlorophyll and other optically related variables using analytical and semi-analytical algorithms. Their spatial resolutions, however, are suitable only for large lakes (> 900 , $1,100$, and 400 ha, respectively). MODIS has been used effectively for water quality studies on some of the Laurentian Great Lakes [77, 78]. Another important problem regarding inland lake applications of these sensors is that their spectral bands were designed for marine waters. They lack a critically important red-edge band needed for most inland water studies.

The next advancement for remote sensing of regional water quality of lakes will come from the European Space Agency (ESA) Sentinel-2 satellites, which at the time of this writing are scheduled for launch in April 2015 (Sentinel-2A) and approximately one year later for Sentinel-2B. Although these satellites were designed primarily for land observations, their improved spatial resolution (10, 20, and 60 m), spectral bands (narrower green and red, red edge, and 3 NIR bands), and temporal coverage (every 3–5 days) will greatly enhance the capabilities to assess optically related water quality characteristics (e.g., chlorophyll, CDOM, SS_{min}) in inland lakes. Landsat 8 and Sentinel-2 have specific SWIR bands selected for atmospheric corrections and cloud screening that will greatly enhance their use for routine monitoring.

An example of water quality maps for chlorophyll a and CDOM created from Sentinel-2 bands is shown in Fig. 5 for the SLRE. In this case, the band information

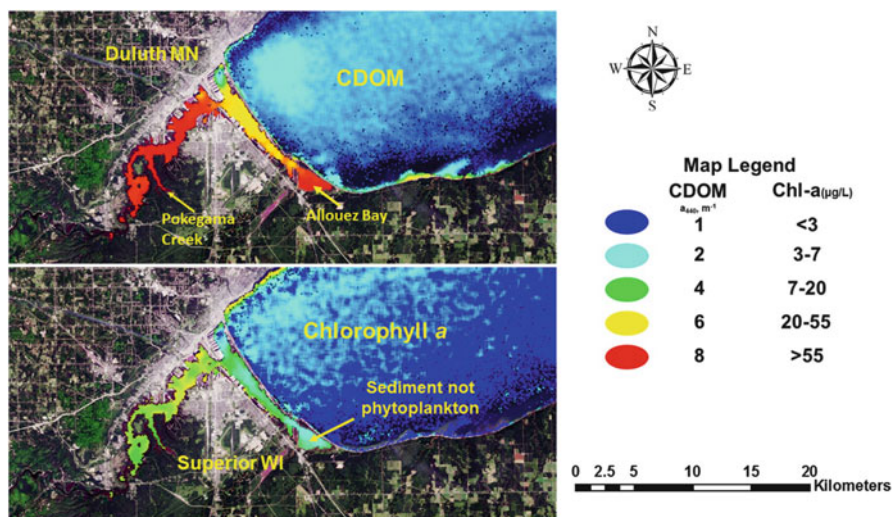


Fig. 5 CDOM and chlorophyll a maps for the St. Louis River Estuary at west end of Lake Superior created from an Aug. 31, 2013, HICO image using simulated Sentinel-2 bands. Spectral characteristics of Sentinel-2 sensor allow discrimination of phytoplankton from SS_{min} in optically complex waters. The SS_{min} dominated waters of Pokegama Creek and Allouez Bay are classified correctly as having low chlorophyll a and high CDOM. Models were developed using data from the St. Louis River Estuary and Lake Superior. Background imagery: Aug 31, 2013, Landsat 8 image

was simulated from imagery obtained by the Hyperspectral Imager for the Coastal Ocean (HICO) on the International Space Station. The spectral characteristics of the simulated Sentinel-2 imagery allowed for accurate measurements of chlorophyll in optically complex waters in contrast to the limitations encountered with Landsat 8 bands (Fig. 3; see Sect. 2.2.5) which misrepresented SS_{\min} as chlorophyll a .

3.1 Empirical and Semi-analytical Approaches to Lake Water Quality Assessment

The algorithms used to retrieve water quality data for inland waters from satellite imagery are empirical to semi-analytical. Empirical algorithms statistically model relationships between measured water quality variables and spectral bands and/or combinations of spectral bands. Strictly empirical algorithms require no understanding of the physics required to model atmospheric and underwater optical properties. Thus, they are relatively simple to perform and are well represented in the literature. This approach is also where many have “oversold” what can be sensed with remote sensing (i.e., when imagery is used for measurements of variables that have no optical properties, such as phosphorus, DOC, or bacteria [23, 24, 79, 80]).

A better approach involves semi-empirical methods, which use bands that are selected based on knowledge of how optically active parameters affect reflectance in various spectral bands. Once such models are identified, they can be applied and used for routine monitoring, as has been done for water clarity assessments of over 20,000 lakes in Minnesota [32], Wisconsin [81], and Michigan [82, 83]. These assessments used field data within a few days of the Landsat image acquisition to calibrate models using the ratio of the Landsat TM1/TM3 bands plus band TM1 as predictor variables. Matthews [35] recently provided a thorough review of the literature on empirical and semi-empirical methods using ORS to measure inland water quality, and that paper should be accessed for further details.

Theoretically, once systemic and atmospheric correction is accurately applied to imagery allowing for a true water-leaving reflectance product, universal algorithms could be developed for specific sensors and water quality variables, which would reduce the need for contemporaneous field data. Unfortunately, accurate atmospheric correction for inland water quality is difficult on a regional basis and needs further development to be operational [1, 84].

Analytical methods are theoretically derived and use complex approaches such as radiative transfer or bio-optical modeling, and semi-analytical methods use analytical techniques that are empirically parameterized with in situ data. Semi-analytical methods to estimate water quality variables are thought by some to be the pathway to global water quality products using ORS [84]. However, many challenges remain with parameterization of the algorithms, and at present there are no successful validated regional assessments using semi-analytical methods in the

literature. Semi-analytical methods are typically region specific and applied to one lake or a few lakes. They require ground-based measurements of the IOPs of each lake for proper model calibration. More recent “adaptable” inversion algorithms [59, 85] are more robust and have the potential to be able to be applied for regional assessments of hundreds to thousands of lakes [84].

4 Regional Lake Water Quality Assessment: Case Studies

4.1 *Water Quality of Inland Lakes*

Early studies using Landsat imagery for water quality assessment were largely exploratory and involved only one or a few lakes [71–76]. An exception is the work of Martin et al. [86], who used semiautomated procedures to assess the trophic status of around 3,000 lakes in Wisconsin using Landsat Multispectral Scanner (MSS) imagery. The first regional assessment using Landsat TM imagery was completed in the Twin Cities Metropolitan Area (Minnesota, USA) on the water clarity of over 500 lakes [87]. Kloiber et al. [31, 88] followed with a temporal assessment and statistical analysis of SD in those same lakes for the 1973 to 1998 period. A decrease in imagery costs corresponding with the launch of Landsat 7 in April 1999, and the establishment of a NASA-funded Upper Midwest Regional Earth Science Applications Center (RESAC) also in 1999, allowed for statewide SD assessments for Minnesota, Wisconsin, and Michigan by the University of Minnesota, University of Wisconsin-Madison, and Michigan State University.

After RESAC funding ended in 2003, Olmanson et al. [32] continued the remote sensing for SD in Minnesota over eight periods from 1975 to 2008. A statistical analysis of the spatial and temporal trends was recently published [89] (see Sect. 4.2). Minnesota lake water clarity data can be accessed in the Lake Browser [90].

The Wisconsin Department of Natural Resources also continued statewide Landsat water clarity assessments on approximately 8,000 Wisconsin lakes annually [81]. All available clear late summer images are being processed for water clarity assessment on an interannual basis (S. Greb, Wisconsin Department of Natural Resources, personal communication, 2014). Wisconsin lake water clarity data can be accessed in the Lakes and AIS Mapping Tool [91].

Since the original water clarity assessment of Michigan lakes in 2002 [82], the United States Geological Survey (USGS) has continued statewide water clarity assessments for ~3,000 lakes. The 2003–2005 and 2007–2008 assessments were documented by Fuller et al. [83]. Since then, the USGS has conducted annual assessments of water clarity in Michigan with 2009–2010 and 2011 completed and 2013–2014 and 2000 assessments underway. Michigan water clarity data can be accessed in the Michigan Lake Water Clarity Interactive Map Viewer [92].

In Maine, McCullough et al. [93] combined watershed characteristics with Landsat data to assess the water clarity of ~1,500 lakes. This approach was also used to investigate temporal trends in water clarity [94], which found that water clarity declined in Maine's lakes during the 1995–2010 period.

4.1.1 Remote Sensing of Great Lakes Water Clarity

The Great Lakes are a good example of water resources for which remote sensing has been used to compensate for the paucity of in situ data. Binding et al. [95] showed the advantage of remote sensing over ground-based monitoring with substantial increase in spatial and temporal coverage. Results using CZCS for the 1979–1985 period and the SeaWiFS for the 1998–2006 period showed seasonal and interannual variability in SD due to phytoplankton blooms, resuspension of bottom sediments, and whiting events. The satellite observations document how long-term impacts can be monitored. The findings indicate that the reduction of nutrient loading and particulate removal by the introduction of zebra mussels through filter feeding significantly changed water clarity for Lake Erie and Lake Ontario. For Lake Erie, SD increased in the eastern basin but decreased in the western basin. SD in Lake Ontario more than doubled to > 4 m after the introduction of zebra mussels. The study also indicated a reduction in the frequency and intensity of whiting events due to the effects of calcium uptake by increased mussel populations.

4.2 *Geospatial and Temporal Analysis of Minnesota's 10,000 Lakes*

Landsat imagery provides a reliable method to obtain comprehensive spatial and temporal coverage of an important water quality variable, water clarity. Traditional ground-based monitoring programs generally target larger recreational lakes and thus are not randomly selected. Using such data to extrapolate to the larger population could lead to biased conclusions [89]. Fortunately, the use of such data to calibrate Landsat imagery for regional assessments allows for the entire population to be studied.

In Minnesota the water clarity database for more than 10,500 lakes for time periods centered around 1985, 1990, 1995, 2000, and 2005 was analyzed statistically for spatial distributions, temporal trends, and relationships with morphometric and watershed factors that potentially affect lake clarity [89]. The analysis found that water clarity is lower in southern and southwestern Minnesota and clearer in the northern and northeastern portions of the state. Temporal trends were detected in ~11 % of the lakes with 4.6 % having improving clarity and 6.2 % decreasing clarity. Small and shallow lakes appeared to be more susceptible to decreasing clarity trends than large and deep lakes. Deep lakes generally had higher clarity

than shallow lakes overall and when grouped by watershed land cover percentages. Lakes in agriculturally dominated ecoregions in southern and western Minnesota were more susceptible to decreasing clarity than the rest of the state. Statewide water clarity remained stable from 1985 to 2005 but decreased in ecoregions where agricultural is the main land use. Water clarity decreased as agriculture and/or urban percentages increased and forested land was associated with higher water clarity.

5 Conclusions

ORS using satellite imagery can be used to measure water quality of inland, marine, and coastal waters. ORS in marine waters is well established with a large investment in several generations of increasingly sophisticated satellite sensors acquiring images with large pixel sizes that are ideal for oceanic and most coastal studies but are too coarse for most inland water bodies. With these systems sophisticated analytical and semi-analytical algorithms have been developed that retrieve chlorophyll levels from the oceans on a routine, global-scale basis.

Remote sensing scientists focusing on inland waters have had to rely on other satellites like Landsat, which have adequate spatial resolution but critical deficiencies in spectral and temporal resolution. The spectral bands used to retrieve chlorophyll levels from oceanic waters do not work in optically complex inland waters. These deficiencies have limited development of retrieval algorithms for inland water quality variables by satellite imagery mostly to empirical and semi-empirical approaches.

Therefore, use of remote sensing for regional inland water quality has progressed slowly since the launch of the first Landsat satellite in 1972. Although there have been many successful regional water quality assessments, these have largely been limited to water clarity due to the available spectral bands and/or to only very large lakes (due to the large pixel size of sensors designed to study the oceans). Landsat 8 (launched in 2013) has some significant improvements over its predecessors, but its spectral and temporal characteristics remain largely unchanged, except for a shorter wavelength blue band. The next big advancement for remote sensing of regional water quality of lakes will come from the ESA Sentinel-2 and Sentinel-3 satellites. Improvements in spectral and temporal characteristics of these satellites will allow for better characterization of chlorophyll, CDOM, and SS_{min} in optically complex waters.

For effective lake management, it is essential to have long-term water quality information on a synoptic scale. Combining Landsat and Sentinel satellite imagery will greatly improve the ability to acquire imagery when needed and should significantly improve the utility and usefulness of ORS for water resource managers. Landsat 8 and Sentinel-2 imagery can be used for the assessment of all lakes, and Sentinel-3 can be used for large lakes more often with its higher temporal resolution. Once reliable water quality products can be produced in a timely fashion

on a regional basis, their adoption and use by resource managers should increase significantly. The increased use of remote sensing will greatly improve the management of our water resources and should ultimately lead to better remote sensing systems for monitoring these important natural resources.

Acknowledgments We gratefully acknowledge the support from the University of Minnesota Agricultural Experiment Station, project MIN-042-056, and the “U-Spatial” project. P.L.B. received support from a Professional Development for Retirees grant from the University of Minnesota Office of the Vice President for Research and Retirees Association.

References

1. Olmanson LG, Brezonik PL, Bauer ME (2011) Evaluation of medium to low resolution satellite imagery for regional lake water quality assessments. *Water Resour Res* 47(9), W09515. doi:[10.1029/2011WR011005](https://doi.org/10.1029/2011WR011005)
2. O’Reilly JE, Maritorena S, Mitchell BG, Siegel DA, Carder KL, Garver SA, Kahru M, McClain C (1998) Ocean color chlorophyll algorithms for SeaWiFS. *J Geophys Res* 103: 24937–24953
3. Franz BA, Bailey SW, Eplee RE, Feldman GC, Kwiatkowska E, McClain C, Meister G, Patt FS, Werdell PJ (2005) The Continuity of ocean color measurements from SeaWiFS to MODIS. In: Butler JJ (ed) *Earth observing lake systems: X*. Proceedings SPIE, vol 5882, The International Society for Optical Engineering, pp 49–60
4. Kutser T, Pierson DC, Kallio KY, Reinart A, Sobek S (2005) Mapping lake CDOM by satellite remote sensing. *Remote Sens Environ* 94:535–540
5. GEO (2007) Inland and nearshore coastal water quality remote sensing. In: Bauer M, Dekker A, DiGiacomo P, Greb S, Gitelson A, Herlevi A, Kutser T (eds) *GEO Group on Earth Observation Workshop Final Report*, 27–29 March 2007, Geneva, p 32
6. Gitelson AA, Gurlin D, Moses WJ, Barrow T (2009) A bio-optical algorithm for the remote estimation of the chlorophyll a concentration in case 2 waters. *Environ Res Lett* 4(4):5. doi:[10.1088/1748-9326/4/4/045003](https://doi.org/10.1088/1748-9326/4/4/045003)
7. Moore GF, Aiken J, Lavender SJ (1999) The atmospheric correction of water colour and the quantitative retrieval of suspended particulate matter in Case II waters: application to MERIS. *Int J Remote Sens* 20(9):1713–1733
8. Bukata RP (2013) Retrospection and introspection on remote sensing of inland water quality: “Like Déjà Vu all over again”. *J Great Lakes Res* 39(Suppl):2–5
9. Mobley CD (1994) Optical properties of water. In: Bass M (ed) *Handbook of optics*. McGraw-Hill, New York, p 1152
10. Devred E, Turpie KR, Moses W, Klemas VV, Moisan T, Babin M, Toro-Farmer G, Forget MH, Jo YH (2013) Future retrievals of water column bio-optical properties using the Hyperspectral Infrared Imager (HypIRI). *Remote Sens* 5:6812–6837. doi:[10.3390/rs5126812](https://doi.org/10.3390/rs5126812)
11. Kutser T, Herlevi A, Kallio K, Arst H (2001) A hyperspectral model for interpretation of passive optical remote sensing data from turbid lakes. *Sci Total Environ* 268:47–58
12. Carlson RE (1977) A trophic state index for lakes. *Limnol Oceanogr* 22:361–369
13. Brezonik PL (1978) Effect of organic color and turbidity on Secchi disk transparency. *J Fish Res Board Can* 35:1410–1416
14. Preisendorfer RW (1986) Secchi disk science: visual optics of natural waters. *Limnol Oceanogr* 31:909–926
15. Austin RW, Petzold T (1981) The determination of the diffuse attenuation coefficient of sea water using the Coastal Zone Color Scanner. *Oceanogr Space* 13:239–256

16. Fichot C, Sathyendranath S, Miller WL (2008) SeaUV and SeaUVC, algorithms for the retrieval of UV/Visible diffuse attenuation coefficients from ocean colour. *Remote Sens Environ* 112: 1584–1602
17. Doerffer R, Schiller H (2008) MERIS lake water algorithm for BEAM ATBD, GKSS Research Center, Geesthacht, Version 1.0, 10 June 2008
18. Doerffer R, Schiller H (2008) MERIS regional, coastal and lake case 2 water project— atmospheric correction ATBD, GKSS Research Center, Geesthacht, Version 1.0, 18 May 2008
19. The European Space Agency Envisat Project (2014) Brockmann Consult: BEAM earth observation toolbox and development platform, documentation pages. <http://www.brockmann-consult.de/cms/web/beam/documentation>. Accessed 28 Aug 2014
20. Klemas V (2013) Remote sensing of emergent and submerged wetlands: an overview. *Int J Remote Sens* 34(18):6286–6320. doi:10.1080/01431161.2013.800656
21. Sawaya K, Olmanson L, Heinert N, Brezonik PL, Bauer ME (2003) Extending satellite remote sensing to local scales: land and water resource monitoring using high-resolution imagery. *Remote Sens Environ* 88:144–156
22. Chipman JW, Olmanson LG, Gitelson AA (2009) Remote sensing methods for lake management: a guide for resource managers and decision-makers. Developed by the North American Lake Management Society in collaboration with Dartmouth College, University of Minnesota, University of Nebraska and University of Wisconsin for the United States Environmental Protection Agency, p 132
23. Vincent RK, McKay RM, Al-Rshaidat MMD, Czajkowski K, Bridgeman T, Savino J (2005) Mapping the bacterial content of surface waters with Landsat TM data: importance for monitoring global surface sources of potable water. In: Proceedings ASPRS Pecora 16: global priorities in land remote sensing, Oct 23–27, 2005, Sioux Falls, SD, p 6
24. Torbick N, Hession S, Hagen S, Wiangwang N, Becker B, Qi J (2013) Mapping inland lake water quality across the Lower Peninsula of Michigan using Landsat TM imagery. *Int J Remote Sens* 34(21):7607–7624. doi:10.1080/01431161.2013.822602
25. Blue Water Satellite, Inc. (2013) White paper: total phosphorus water monitoring using satellite imagery. http://bluewatersatellite.com/resources/js/tinymce/jscripts/tiny_mce/plugins/uploaded/How%20Satellite%20Images%20Provide%20Total%20Phosphorus%20Monitoring%20White%20Paper.pdf. Accessed 28 Aug 2014
26. Bukata RP (2005) Satellite monitoring of inland and coastal water quality retrospection, introspection, future directions. CRC, Boca Raton, p 272
27. Ford TE, Colwell RR, Rose JB, Morse SS, Rogers DJ, Yates TL (2009) Using satellite images of environmental changes to predict infectious disease outbreaks. *Emerg Infect Dis* 15(9): 1341–1346. doi:10.3201/eid1509.081334. <http://wwwnc.cdc.gov/eid/article/15/9/08-1334>
28. Vertucci FA, Likens GE (1989) Spectral reflectance and water quality of Adirondack Mountain region lakes. *Limnol Oceanogr* 34:1656–1672
29. Brezonik PL, Olmanson LG, Finlay JC, Bauer ME (2014) Factors affecting the measurement of CDOM by remote sensing of optically complex inland waters. *Remote Sens Environ* 155. doi:10.1016/j.rse.2014.04.033
30. Spencer RGM, Butler KD, Aiken GD (2012) Dissolved organic carbon and chromophoric dissolved organic matter properties of rivers in the USA. *J Geophys Res* 117, G03001. doi:10.1029/2011JG001928
31. Kloiber SM, Brezonik PL, Olmanson LG, Bauer ME (2002) A procedure for regional lake water clarity assessment using Landsat multispectral data. *Remote Sens Environ* 82:38–47
32. Olmanson LG, Bauer ME, Brezonik PL (2008) A 20-year Landsat water clarity census of Minnesota's 10,000 lakes. *Remote Sens Environ* 112(11):4086–4097. doi:10.1016/j.rse.2007.12.013
33. Chipman JW, Lillesand TM, Schmaltz JE, Leale JE, Nordheim MJ (2004) Mapping lake water clarity with Landsat images in Wisconsin, USA. *Can J Remote Sens* 30:1–7

34. Gitelson A, Garbuzov G, Szilagyi F, Mittenzwey K, Karnieli A, Kaiser A (1993) Quantitative remote sensing methods for real-time monitoring of inland waters quality. *Int J Remote Sens* 14:1269–1295
35. Matthews MW (2011) A current review of empirical procedures of remote sensing in inland and near-coastal transitional waters. *Int J Remote Sens* 32:6855–6899
36. Härmä P, Vepsäläinen J, Hannonen T, Pyhälähti T, Kamari J, Kallio K, Eloheimo K, Koponen S (2001) Detection of water quality using simulated satellite data and semi-empirical algorithms in Finland. *Sci Total Environ* 268:107–121
37. Kallio K, Kutser T, Hannonen T, Koponen S, Pulliainen J, Vepsäläinen J, Pyhälähti T (2001) Retrieval of water quality from airborne imaging spectrometry of various lake types in different seasons. *Sci Total Environ* 268:59–77. doi:10.1016/S0048-9697(00)00685-9
38. Koponen S, Attila J, Pulliainen J, Kallio K, Pyhälähti T, Lindfors A, Rasmus K, Hallikainen M (2007) A case study of airborne and satellite remote sensing of a spring bloom event in the Gulf of Finland. *Cont Shelf Res* 27:228–244. doi:10.1016/j.csr.2006.10.006
39. Senay GB, Shafique NA, Autrey BC, Fulk F, Cormier SM (2001) The selection of narrow wavebands for optimizing water quality monitoring on the Great Miami River, Ohio using hyperspectral remote sensor data. *J Spatial Hydrol* 1:1–22
40. Shafique NA, Autrey BC, Fulk FA, Flotemersch JE (2003) Hyperspectral remote sensing of water quality parameters for large rivers in the Ohio River Basin. In: First interagency conference on research in the watersheds, Benson, Arizona, October 27–30, 2003. USDA Agricultural Research Service, Washington DC
41. Ammenberg P, Flink P, Lindell T, Pierson D, Strombeck N (2002) Bio-optical modelling combined with remote sensing to assess water quality. *Int J Remote Sens* 23(8):1621–1638. doi:10.1080/01431160110071860
42. Olmanson LG, Brezonik PL, Bauer ME (2013) Airborne hyperspectral remote sensing to assess spatial distribution of water quality characteristics in large rivers: the Mississippi River and its tributaries in Minnesota. *Remote Sens Environ* 130:254–265
43. Morel A, Prieur L (1977) Analysis of variations in ocean color. *Limnol Oceanogr* 22:709–722
44. Gitelson A (1992) The peak near 700 nm on reflectance spectra of algae and water: relationships of its magnitude and position with chlorophyll concentration. *Int J Remote Sens* 13(17):3367–3373
45. Moses WJ, Gitelson AA, Perk RL, Gurlin D, Rundquist DC, Leavitt BC, Barrow TM, Brakhage P (2011) Estimation of chlorophyll-a concentration in turbid productive waters using airborne hyperspectral data. *Water Res* 46(4):993–1004. doi:10.1016/j.watres.2011.11.068
46. Duan HT, Zhang YZ, Zhan B, Song KS, Wang ZM (2007) Assessment of chlorophyll-a concentration and trophic state for Lake Chagan using Landsat TM and field spectral data. *Environ Monit Assess* 129:295–308. doi:10.1007/s10661-006-9362-y
47. Gons HJ (1999) Optical teledetection of chlorophyll a in turbid inland waters. *Environ Sci Tech* 33:1127–1132. doi:10.1021/es9809657
48. Mittenzwey K, Gitelson A, Ullrich S, Kondratiev K (1992) Determination of chlorophyll a of inland waters on the basis of spectral reflectance. *Limnol Oceanogr* 37:147–149
49. Menken K, Brezonik PL, Bauer ME (2006) Influence of chlorophyll and humic color on reflectance spectra of lakes: implications for measurement of lake-water properties by remote sensing. *Lake Reserv Manag* 22(3):179–190
50. Moses WJ, Gitelson AA, Berdnikov S, Povazhnyy V (2009) Satellite estimation of chlorophyll-a concentration using the red and NIR bands of MERIS—the Azov Sea case study. *IEEE Geosci Remote Sens Lett* 6:845–849. doi:10.1109/LGRS.2009.2026657
51. Minnesota Department of Natural Resources (2014) LakeFinder. <http://www.dnr.state.mn.us/lakefind/index.html>. Accessed 28 Aug 2014
52. Schalles J, Yacobi Y (2000) Remote detection and seasonal patterns of phycocyanin, carotenoid and chlorophyll pigments in eutrophic waters. *Archives Hydrobiology, special issues. Adv Limnol* 55:153–168

53. Randolph KL, Wilson J, Tedesco L, Li L, Pascual L, Soyeux E (2008) Hyperspectral remote sensing of cyanobacteria in turbid productive water using optically active pigments, chlorophyll a and phycocyanin. *Remote Sens Environ* 112:4009–4019
54. Vincent RK, Qin X, McKay RM, Miner J, Czajkowski K, Savino J, Bridgeman T (2004) Phycocyanin detection from Landsat TM data for mapping cyanobacterial blooms in Lake Erie. *Remote Sens Environ* 89(3):381–392
55. Wynne TT, Tomlinson MC, Warner RA, Tester PA, Dyble J, Fahnensteil GL (2008) Relating spectral shape to cyanobacterial blooms in the Laurentian Great Lakes. *Int J Remote Sens* 29:3665–3672
56. Wynne TT, Stumpf RP, Tomlinson MC, Dyble J (2010) Characterizing a cyanobacterial bloom in western Lake Erie using satellite imagery and meteorological data. *Limnol Oceanogr* 55:2025–2036
57. Wynne TT, Stumpf RP, Tomlinson MC, Fahnensteil GL, Dyble J, Schwab DJ, Joseph-Joshi S (2013) Evolution of a cyanobacteria bloom forecast system in western Lake Erie: development and initial evaluation. *J Great Lakes Res* 39:90–99. doi:[10.1016/j.jglr.2012.10.003](https://doi.org/10.1016/j.jglr.2012.10.003)
58. Lunetta RS, Schaeffer BA, Stumpf RP, Keith D, Jacobs SA, Murphy MS (2014) Evaluation of cyanobacteria cell count detection derived from MERIS imagery across the eastern USA. *Remote Sens Environ*. doi:[10.1016/j.rse.2014.06.008](https://doi.org/10.1016/j.rse.2014.06.008)
59. Brando VE, Dekker AG, Park YJ, Schroeder T (2012) Adaptive semianalytical inversion of ocean color radiometry in optically complex waters. *Appl Optics* 51:2808–2833
60. Carder KL, Chen FR, Lee ZP, Hawes SK, Kamykowski D (1999) Semianalytic moderate-resolution imaging spectrometer algorithms for chlorophyll a and absorption with bio-optical domains based on nitrate-depletion temperatures. *J Geophys Res Oceans* 104:5403–5421
61. Hoge FE, Lyon PE (1996) Satellite retrieval of inherent optical properties by linear matrix inversion of oceanic radiance models: an analysis of model and radiance measurement errors. *J Geophys Res Oceans* 101:16631–16648
62. Zhu W, Yu Q, Tian YQ, Chen RF, Gardner GB (2011) Estimation of chromophoric dissolved organic matter in the Mississippi and Atchafalaya river plume regions using above-surface hyperspectral remote sensing. *J Geophys Res* 116, C02011. doi:[10.1029/2010JC006523](https://doi.org/10.1029/2010JC006523)
63. Ficek D, Zapadka T, Dera J (2011) Remote sensing reflectance of Pomeranian lakes and the Baltic. *Oceanologia* 53:959–970
64. Xiao YH, Sara-Aho T, Hartikainen H, Vähätalo AV (2013) Contribution of ferric iron to light absorption by chromophoric dissolved organic matter. *Limnol Oceanogr* 58:653–662
65. Köhler SJ, Kothawala D, Futter MN, Liungman O, Tranvik L (2013) In-lake processes offset increased terrestrial inputs of dissolved organic carbon and color to lakes. *PLoS ONE* 8(8):e70598. <http://dx.doi.org/10.1371/j.pone.0070598>
66. Müller RA, Futter MN, Sobek S, Nisell J, Bishop K, Weyhenmeyer GA (2013) Water renewal along the aquatic continuum offsets cumulative retention by lakes: implications for the character of organic carbon in boreal lakes. *Aquat Sci* 75:535–545
67. Helms JR, Stubbins A, Ritchie JD, Minor EC, Kieber DJ, Mopper K (2008) Absorption spectral slopes and slope ratios as indicators of molecular weight, source, and photobleaching of chromophoric dissolved organic matter. *Limnol Oceanogr* 53:955–969
68. Williamson CE, Brentrup JA, Zhang J, Renwick WH, Hargreaves BR, Knoll LB, Overholt EP, Rose KC (2014) Lakes as sensors in the landscape: optical metrics as scalable sentinel responses to climate change. *Limnol Oceanogr* 59:840–850
69. Pace ML, Cole JJ (2002) Synchronous variation of dissolved organic carbon and color in lakes. *Limnol Oceanogr* 47:333–342
70. Sobek S, Tranvik LJ, Prairie YT, Kortelainen P, Cole JJ (2007) Patterns and regulation of dissolved organic carbon: an analysis of 7,500 widely distributed lakes. *Limnol Oceanogr* 52:1208–1219
71. Brown D, Warwick R, Skaggs R (1977) Lake condition in east central Minnesota. Minnesota Land Management Information System Report 5022. Center for Urban and Regional Affairs, University of Minnesota, Minneapolis

72. Dekker AG, Peters SWM (1993) The use of the thematic mapper for the analysis of eutrophic lakes—a case-study in the Netherlands. *Int J Remote Sens* 14(5):799–821
73. Lathrop RG (1992) Landsat Thematic Mapper monitoring of turbid inland water quality. *Photogramm Eng Remote Sens* 58:465–470
74. Lathrop RG, Lillesand TM, Yandell BS (1991) Testing the utility of simple multivariate Thematic Mapper calibration algorithms for monitoring turbid inland waters. *Int J Remote Sens* 12: 2045–2063
75. Lillesand TM, Johnson WL, Deuell RL, Lindstrom OM, Meisner DE (1983) Use of Landsat data to predict the trophic state of Minnesota lakes. *Photogramm Eng Remote Sens* 49: 219–229
76. Ritchie JC, Cooper CM, Schiebe FR (1990) The relationship of MSS and TM digital data with suspended sediments, chlorophyll and temperature in Moon Lake, Mississippi. *Remote Sens Environ* 33:137–148
77. Shuchman R, Leshkevich G, Hat C, Pozdnyakov D, Korosov A (2008) Development of a robust hydro-optical model for the Great Lakes for the extraction of chlorophyll, dissolved organic carbon and suspended minerals from MODIS satellite data. In: IAGLR 51st Annual Conference on Great Lakes Research, 19–23 May 2008, Petersborough, ON
78. Grimm A (2013) Satellite Remote Sensing-Based Coastal and Nearshore Monitoring Research at MTRI. Michigan Tech Research Institute, Michigan Technological University. <http://glc.org/files/projects/lmmcc/lmmcc-20130418-Grimm-lmmccnemol.pdf>. Accessed 28 Aug 2014
79. Rogers RH (1975) Application of Landsat to the surveillance and control of lake eutrophication in the Great Lakes Basin. Type II Report for the Period of August 11 through November 11, 1975, Prepared for Goddard Space Flight Center, p 55
80. McKeon JB, Rogers RH (1976) Water quality map of Saginaw Bay from computer processing of Landsat-2 data. Special Report Prepared for Goddard Space Flight Center, p 6
81. Greb SR, Martin AA, Chipman JW (2009) Water Clarity Monitoring of Lakes in Wisconsin, USA using Landsat. In: *Proceeding of 33rd International Symposium of Remote Sensing of the Environment*, 4–8 May 2009, Stresa
82. Fuller LM, Aichele SS, Minnerick RJ (2004) Predicting water quality by relating Secchi-disk transparency and chlorophyll *a* measurements to Satellite Imagery for Michigan Inland Lakes, August 2002: U.S. Geological Survey Scientific Investigations Report 2004–5086
83. Fuller LM, Jodoin RS, Minnerick RJ (2011) Predicting lake trophic state by relating Secchi-disk transparency measurements to Landsat-satellite imagery for Michigan inland lakes, 2003–05 and 2007–08: U.S. Geological Survey Scientific Investigations Report 2011–5007, p 36
84. Malthus TJ, Hestir EL, Dekker AG, Brando VE (2012) The case for a global inland water quality product. In: *Proceedings, IEEE International Geoscience and Remote Sensing Symposium (IGARSS)*, 22–27 July 2012, 5234–5237. doi:10.1109/IGARSS.2012.6352429
85. Campbell G, Phinn SR, Dekker AG, Brando VE (2011) Remote sensing of water quality in an Australian tropical freshwater impoundment using matrix inversion and MERIS image. *Remote Sens Environ* 115:2403–2414
86. Martin RH, Boebel EO, Dunst RC, Williams OD, Olsen MV, Merideth RW Jr, Scarpace FL (1983) Wisconsin lakes—a trophic assessment using Landsat digital data. Wisconsin Lake Classification Survey Project, S00536601, p 294
87. Olmanson LG (1997) Satellite remote sensing of the trophic state conditions of lakes in the Twin Cities Metropolitan Area. University of Minnesota, St. Paul
88. Kloiber SM, Brezonik PL, Bauer ME (2002) Application of Landsat imagery to regional-scale assessments of lake clarity. *Water Res* 36:4330–4340
89. Olmanson LG, Brezonik PL, Bauer ME (2013) Geospatial and temporal analysis of a 20-year record of Landsat-based water clarity in Minnesota’s 10,000 lakes. *J Am Water Resour Assoc* 50:748–761. doi:10.1111/jawr.12138
90. University of Minnesota (2011) Remote Sensing and Geospatial Analysis Laboratory. Remote Sensing of Water, Lake Browser. <http://water.umn.edu/>. Accessed 28 Aug 2014
91. Wisconsin Department of Natural Resources (2014) Lakes & AIS Mapping Tool. <http://dnmmaps.wi.gov/SL/?Viewer=Lakes%20and%20AIS%20Viewer>. Accessed 28 Aug 2014

92. U.S. Geologic Survey (2014) Michigan Water Science Center. Michigan Lake Water Clarity Interactive Map Viewer. <http://miwebmapper.er.usgs.gov/cmilakers/>. Accessed 28 Aug 2014
93. McCullough IM, Loftin CS, Sader SA (2012) Combining lake and watershed characteristics with Landsat TM data for remote estimation of regional lake clarity. *Remote Sens Environ* 123:109–115
94. McCullough IM, Loftin CS, Sader SA (2013) Landsat imagery reveals declining clarity of Maine's lakes during 1995–2010. *Freshw Sci* 32(3):741–752. doi:[10.1899/12-070.1](https://doi.org/10.1899/12-070.1)
95. Binding CE, Jerome JH, Bukata RP, Booty WG (2007) Trends in water clarity of the Lower Great Lakes from remotely sensed aquatic color. *J Great Lakes Res* 33:828–841. doi:[10.3394/0380-1330\(2007\)33\[828:TIWCOT\]2.0.CO;2](https://doi.org/10.3394/0380-1330(2007)33[828:TIWCOT]2.0.CO;2)